Acta Crystallographica Section A
Foundations of Crystallography
ISSN 0108-7673

Received 25 January 2005
Accepted 7 March 2005

A transition path for the pressure-induced wurtzite- to NaCl-type transformation described in $Pna2_1$

H. Sowa

Institut für Mineralogie, Petrologie und Kristallographie, Philipps-Universität Marburg, Hans-Meerwein-Strasse, D-35032 Marburg, Germany. Correspondence e-mail: heidrun.sowa@t-online.de

Quite recently, two further mechanisms for the pressure-induced transition from the wurtzite to the NaCl type were proposed [Shimojo *et al.* (2004). *Phys. Rev. B*, **70**, 184111-1–6] but no symmetry information was given. It will be shown that a slight modification of one of the assumed transition pathways allows a crystallographic description on the basis of a deformation of a heterogeneous 4-connected sphere packing in $Pna2_1$. All investigations were done with the help of the corresponding homogeneous packing in *Pnma* where the transition may be described as a deformation of a lonsdaleite configuration into a cubic primitive lattice *cP*. During the transformation, all sphere contacts are maintained. The new transition model is compared with the well known $Cmc2_1$ mechanism. Further related mechanisms can also be derived.

1. Introduction

At ambient conditions, most of the four-coordinated *AB* compounds crystallize with a structure belonging either to the zinc-blende or to the wurtzite type. Under high pressure, many of these compounds undergo a phase transition to a modification with an NaCl-type structure. During the last years, such phase transitions have received considerable interest, and especially the underlying transition mechanisms have attracted much attention. Although these transformations are usually termed 'reconstructive' because they are accompanied by large volume discontinuities, models for diffusionless transitions were suggested. These models involve cooperative shifts of the atoms while the metric changes simultaneously. For the phase transformations between the zinc-blende and the NaCl type, two different mechanisms have been described that do not require any breaking of bonds (*cf.* Sowa, 2000*b*, 2003; Shimojo *et al.*, 2000; Wilson *et al.*, 2002).

The transformation between the wurtzite and the NaCl type has already been described by Corll (1967) as a continual deformation. Further transition models were developed later (Tolbert & Alivisatos, 1995; Sharma & Gupta, 1998; Knudson *et al.*, 1999; Limpijumnong & Lambrecht, 2001*a*). However, all these models may be explained by the same pattern of atomic displacements (Wilson & Madden, 2002). As an investigation with crystallographic methods reveals (Sowa, 2001), such a transition can be described as a deformation of a heterogeneous sphere packing *via* an intermediate phase with symmetry $Cmc2_1$. During the transformation, the atoms are shifted *e.g.* by vectors $\pm\frac{1}{12}\sqrt{3}\mathbf{a} \pm \frac{1}{16}\mathbf{c}$ within one of the $\{1\bar{2}0\}$ planes of the wurtzite-structure type ($P6_3mc$).

In a very recent paper, Shimojo *et al.* (2004) studied the phase transformation in CdSe by molecular dynamics simulations. They presented two further transition paths for the wurtzite- to NaCl-type transformation. The first one involves movements of the atoms within the (100) planes of the wurtzite structure type: every other double layer of atoms is shifted along the [010] direction.[1] According to the second new mechanism, the atoms in the (100) planes are also shifted along [010], but the relative shifts between adjacent double layers are very different. The calculations of Shimojo *et al.* (2004) reveal very similar energy barriers of about 0.13 eV/pair for all three transition paths.

The present paper demonstrates that a slight modification of the first additional mechanism proposed by Shimojo *et al.* (2004) enables a crystallographic description of the phase transition from the wurtzite to the NaCl type.

2. Symmetry relations between the wurtzite and the NaCl type

For the investigations described below, the same procedure was used as in previous papers on the derivation of possible transition mechanisms (Sowa, 2000*a*,*b*; 2001, 2003). Both the wurtzite-type ($P6_3mc$) and the NaCl-type structures ($Fm\bar{3}m$) were considered as heterogeneous sphere packings. If all atoms in these structures are assumed to be equivalent, the corresponding sphere packings are homogeneous. The resulting structure with four-coordinated atoms belongs to the lonsdaleite type ('hexagonal diamond') with symmetry $P6_3/mmc$ 4(*f*). An ideal lonsdaleite configuration with axial ratio $c/a = \frac{2}{3}\sqrt{6} \cong 1.633$ refers to a sphere packing of type

[1] In their publication, the authors used an unusual nomenclature for the crystallographic directions and planes. In the present paper, the crystallographic three-index symbols are given.

Table 1
Sphere packings surrounding 4/6/*h*2 in *Pnma* and their highest possible symmetries.

Sphere-packing types are symbolized by *k*/*m*/*fn* according to a proposal by Fischer (1973): *k* is the number of contacts per sphere, *m* is the size of the shortest mesh, *f* indicates the highest crystal family for packings of that type, *n* is an arbitrary number.

Sphere-packing type	Sphere-packing parameters in *Pnma*	Highest possible symmetry and parameters at minimal density
5/4/*h*5[d]	$x=\frac{1}{3}$, $y=0$, $z=0$; $a/b=\frac{3}{2}$, $c/b=\frac{1}{2}\sqrt{3}$	*P*6/*mmm* 2(*c*) $\frac{1}{3},\frac{2}{3},0$; $c/a=\frac{1}{2}\sqrt{3}$
5/4/*t*6[b]	$x=\frac{1}{4}$, $y=\frac{1}{16}$, $z=0$; $a/b=\frac{1}{2}\sqrt{2}$, $c/b=\frac{1}{2}\sqrt{2}$ $x=\frac{3}{8}$, $y=\frac{1}{16}$, $z=\pm\frac{1}{4}$, $a/b=1$, $c/b=\frac{1}{2}$	*I*4/*mmm* 4(*e*) $0,0,z$; $z=\frac{3}{16}$; $c/a=2$
6/3/*o*2[c]	$x=\frac{1}{64}(13+\sqrt{105})$, $y=\frac{1}{16}(\sqrt{105}-9)$, $z=0$; $a/b=\frac{3}{8}\sqrt{15}-\frac{1}{8}\sqrt{7}$, $c/b=\frac{13}{8}-\frac{1}{8}\sqrt{105}$	*Cmcm* 8(*f*) $0,y,z$; $y=\frac{1}{64}(19-\sqrt{105})$, $z=\frac{1}{16}(\sqrt{105}-9)$; $a/b=\frac{1}{4}\sqrt{15}-\frac{1}{4}\sqrt{7}$, $c/b=\frac{1}{16}(3\sqrt{15}+\sqrt{7})$
6/3/*o*5[e]	$x=\frac{1}{128}(51-\sqrt{105})$, $y=\frac{1}{16}(\sqrt{105}-9)$, $z=\pm\frac{1}{32}(\sqrt{105}-5)$; $a/b=\frac{5}{16}\sqrt{35}-\frac{11}{16}\sqrt{3}$, $c/b=\frac{1}{4}\sqrt{21}-\frac{1}{4}\sqrt{5}$	*Pnma* 8(*d*)
6/4/*c*1[a]	$x=\frac{1}{4}$, $y=0$, $z=0$; $a/b=1$, $c/b=1$; $x=\frac{3}{8}$, $y=0$, $z=\pm\frac{1}{4}$; $a/b=\sqrt{2}$, $c/b=\frac{1}{2}\sqrt{2}$	*Pm*$\bar{3}$*m* 1(*a*) 0,0,0
7/3/*t*5[b]	$x=\frac{3}{4}-\frac{1}{4}\sqrt{3}$, $y=0$, $z=\pm\frac{1}{4}\sqrt{3}-\frac{1}{4}$; $a/b=\frac{1}{4}\sqrt{6}+\frac{1}{4}\sqrt{2}$, $c/b=\frac{1}{4}\sqrt{6}+\frac{1}{4}\sqrt{2}$	*P*4/*mbm* 4(*g*) $x,x+\frac{1}{2},0$; $x=\frac{1}{4}\sqrt{3}-\frac{1}{4}$; $c/a=\frac{1}{2}\sqrt{6}-\frac{1}{2}\sqrt{2}$
7/3/*o*1[c]	$x=\frac{1}{2}\sqrt{3}-\frac{1}{2}$, $y=0$, $z=0$; $a/b=1+\frac{1}{2}\sqrt{3}$, $c/b=\frac{1}{2}$	*Cmmm* 4(*g*) $x,0,0$; $x=1-\frac{1}{2}\sqrt{3}$; $a/b=2+\sqrt{3}$, $c/b=1$
7/3/*o*5[e]	$x=\frac{3}{8}$, $y=\frac{1}{2}\sqrt{7}-\frac{5}{4}$, $z=\pm\frac{1}{4}$; $a/b=6-2\sqrt{7}$, $c/b=\sqrt{(2\sqrt{7}-5)}$; $x=\frac{3}{8}$, $y=\frac{1}{2}\sqrt{7}-\frac{5}{4}$, $z=\pm\frac{1}{4}$; $a/b=2\sqrt{(2\sqrt{7}-5)}$, $c/b=3-\sqrt{7}$	*Immm* 4(*e*) $x,0,0$; $x=\frac{3}{2}-\frac{1}{2}\sqrt{7}$; $a/b=2\sqrt{2}$, $c/b=\sqrt{(1+\frac{1}{2}\sqrt{7})}$
7/3/*o*7[e]	$x=\frac{1}{4}$, $y=\frac{1}{2}\sqrt{7}-\frac{5}{4}$, $z=\pm\frac{1}{36}(4\sqrt{7}-7)$; $a/b=\frac{2}{3}\sqrt{(26\sqrt{7}-68)}$, $c/b=\sqrt{7}-2$	*Pnma* 8(*d*)
8/3/*o*2[c]	$x=\frac{9}{32}$, $y=\frac{3}{28}$, $z=0$; $a/b=\frac{8}{49}\sqrt{7}$, $c/b=\frac{4}{49}\sqrt{21}$	*Cmcm* 8(*f*) $0,y,z$; $y=\frac{7}{32}$, $z=\frac{3}{28}$; $a/b=\frac{1}{2}\sqrt{3}$, $c/b=\frac{7}{8}\sqrt{7}$
8/3/*o*4[e]	$x=\frac{23}{64}$, $y=\frac{3}{28}$, $z=\pm\frac{5}{28}$; $a/b=\frac{16}{49}\sqrt{3}$, $c/b=\frac{2}{7}$	*Pnma* 8(*d*)
8/3/*h*4[d]	$x=\frac{1}{4}$, $y=0$, $z=\pm\frac{1}{8}$; $a/b=\frac{1}{2}\sqrt{3}$, $c/b=1$; $x=\frac{3}{8}$, $y=0$, $z=\pm\frac{1}{4}$; $a/b=1$, $c/b=\frac{1}{2}\sqrt{3}$; $x=\frac{3}{8}$, $y=0$, $z=\pm\frac{1}{4}$; $a/b=\sqrt{3}$, $c/b=\frac{1}{2}$	*P*6/*mmm* 1(*a*) 0,0,0; $c/a=1$
9/3/*t*2[b]	$x=\frac{1}{4}$, $y=\frac{1}{4}\sqrt{2}-\frac{1}{4}$, $z=0$; $a/b=\sqrt{2}-1$, $c/b=\sqrt{2}-1$; $x=\frac{3}{8}$, $y=\frac{1}{4}\sqrt{2}-\frac{1}{4}$, $z=\pm\frac{1}{4}$; $a/b=2-\sqrt{2}$, $c/b=1-\frac{1}{2}\sqrt{2}$	*I*4/*mmm* 4(*e*) $0,0,z$; $z=\frac{1}{2}-\frac{1}{4}\sqrt{2}$; $c/a=1-\frac{1}{2}\sqrt{2}$
10/3/*h*2[d]	$x=\frac{1}{3}$, $y=\frac{1}{4}\sqrt{6}-\frac{1}{2}$, $z=0$; $a/b=\frac{3}{2}\sqrt{3}-\frac{3}{2}\sqrt{2}$, $c/b=\frac{3}{2}-\frac{3}{2}\sqrt{6}$	*P*6$_3$/*mmc* 4(*f*) $\frac{1}{3},\frac{2}{3},z$; $z=\frac{1}{4}\sqrt{6}-\frac{1}{2}$; $c/a=2+\frac{2}{3}\sqrt{6}$

References: (*a*) Fischer, 1973; (*b*) Fischer, 1991; (*c*) Sowa, 2001; (*d*) Sowa *et al.*, 2003; (*e*) this work.

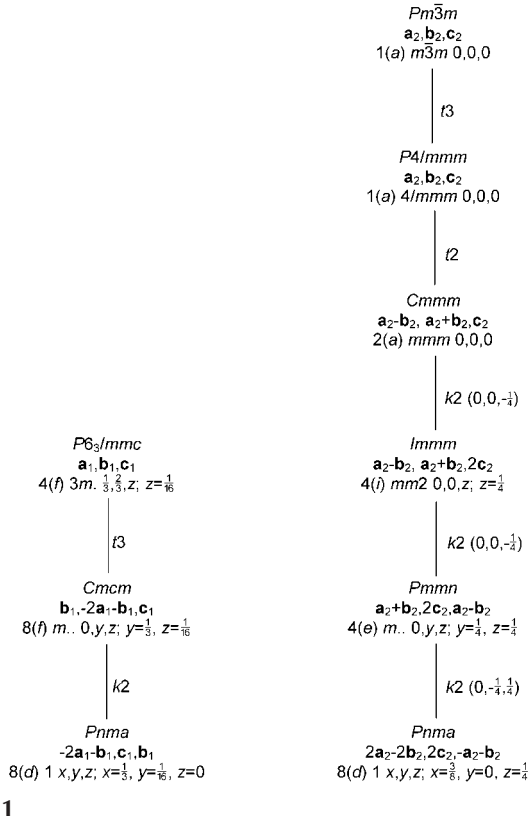

Figure 1
Symmetry relations between a lonsdaleite configuration and a cubic primitive lattice.

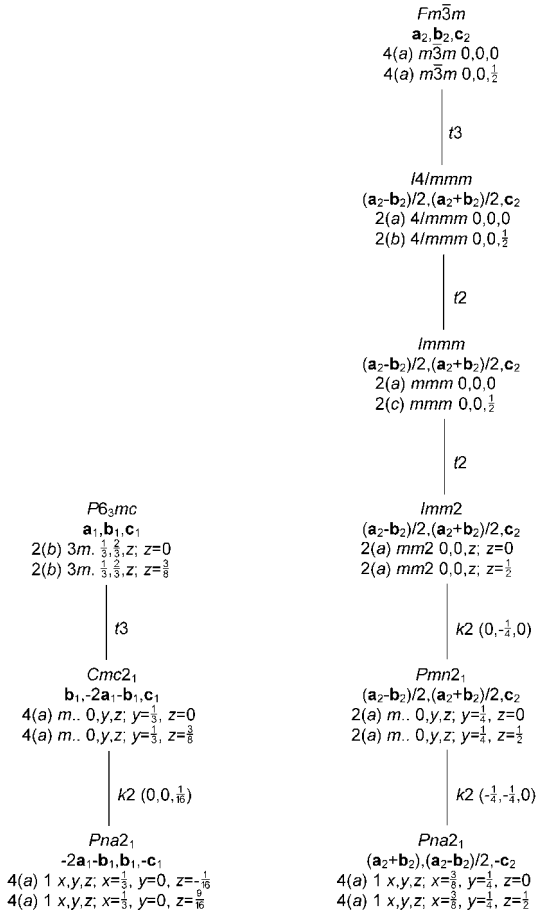

Figure 2
Symmetry relations between the structure types of wurtzite and NaCl.

4/6/*h*2 (Sowa *et al.*, 2003). The analogue of an NaCl-type structure corresponds to a primitive cubic lattice (*cP*, $Pm\bar{3}m$ 1*a*) and to a sphere packing of type 6/4/*c*1 (Fischer, 1973). The lattice parameter *a* of the $Pm\bar{3}m$ structure is half that of the original space group $Fm\bar{3}m$. On account of the easier calculations, all investigations were made using homogeneous sphere packings and the results were transferred to heterogeneous configurations.

The pattern of the relative atomic displacements for the first transition model from a wurtzite- to an NaCl-type structure proposed by Shimojo *et al.* (2004) shows the symmetry $Pna2_1$. Provided that no bonds are broken during the phase transformation, a continuous deformation of a sphere packing of type 4/6/*h*2 into a sphere packing of type 6/4/*c*1 should be possible in the supergroup *Pnma* of $Pna2_1$. The appropriate subgroup relationships (Fig. 1) were derived by using the tables by Müller (2004). Both space groups $P6_3/mmc$ and $Pm\bar{3}m$ have a common subgroup *Pnma*. The lonsdaleite configuration exists in the general position of *Pnma* 8(*d*) *x*, *y*, *z* with $x = \frac{1}{3}$, $y = \frac{1}{16}$, $z = 0$ and $a_o = \sqrt{3}a_h$, $b_o = c_h$, $c_o = a_h$, $a_o/b_o = \frac{3}{4}\sqrt{2} \cong 1.061$ and $c_o/b_o = \frac{1}{4}\sqrt{6} \cong 0.612$. *cP* occurs as a limiting complex at 8(*d*) *x*, *y*, *z* with $x = \frac{3}{8}$, $y = 0$, $z = \frac{1}{4}$ and $a_o = 2\sqrt{2}a_c$, $b_o = 2a_c$, $c_o = \sqrt{2}a_c$, $a_o/b_o = \sqrt{2} \cong 1.414$ and $c_o/b_o = \frac{1}{2}\sqrt{2} \cong 0.707$.

The analogous symmetry reduction for the corresponding *AB* compounds is shown in Fig. 2. The ideal wurtzite-type arrangement is obtained in $Pna2_1$ if the atoms occupy the position 4(*a*) *x*, *y*, *z* with $x = \frac{1}{3}$, $y = 0$, $z = -\frac{1}{16}$ and $x = \frac{1}{3}$, $y = 0$, $z = \frac{9}{16}$, respectively. In addition, $a_o = \sqrt{3}a_h$, $b_o = a_h$, $c_o = c_h$, $a_o/b_o = \sqrt{3} \cong 1.732$ and $c_o/b_o = \frac{2}{3}\sqrt{6} \cong 1.633$ must be fulfilled. For the undistorted NaCl-type configuration, the atoms are located at position 4(*a*) *x*, *y*, *z* with $x = \frac{3}{8}$, $y = \frac{1}{4}$, $z = 0$ and $x = \frac{3}{8}$, $y = \frac{1}{4}$, $z = \frac{1}{2}$, respectively, while $a_o = \sqrt{2}a_c$, $b_o = \frac{1}{2}\sqrt{2}a_c$, $c_o = a_c$, $a_o/b_o = 2$ and $c_o/b_o = \sqrt{2} \cong 1.414$.

This transition path for the wurtzite- to NaCl-type transformation has been overlooked before (Perez-Mato *et al.*, 2003; Sowa, 2005) because only those subgroups of $P6_3mc$ have been considered that are not subgroups of $Cmc2_1$, the group of the intermediate phase proposed by Sowa (2001). However, $Pna2_1$ is a subgroup of $Cmc2_1$ and likewise *Pnma* is a subgroup of *Cmcm*.

3. The lonsdaleite-type to *cP* and the corresponding wurtzite- to NaCl-type transition

The lattice complex *Cmcm* 8(*f*) where the first described transition path can be realized (Sowa, 2001) occurs as a limiting complex of *Pnma* 8(*d*) (Engel *et al.*, 1984).

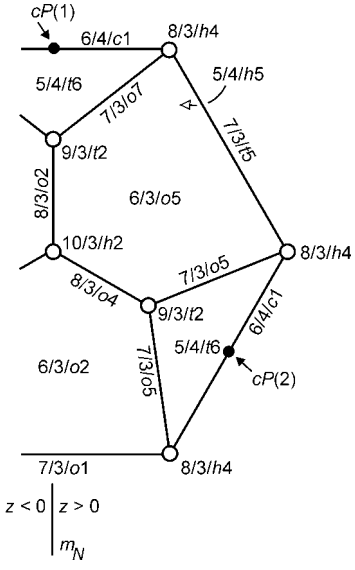

Figure 3
Schlegel diagram showing the sphere-packing types at the boundary of the region of 4/6/*h*2 in *Pnma* 8(*d*). Faces correspond to sphere-packing types with two-dimensional parameter regions, lines and open circles to those with one- and zero-dimensional regions, respectively. Solid circles mark the positions of ideal *cP* arrangements. Sphere packings with $z < 0$ are equivalent to those with $z > 0$ with respect to the Euclidean normalizer $N_E(Pnma) = Pmmm(2\mathbf{a}, 2\mathbf{b}, 2\mathbf{c})$ (Koch *et al.*, 2002).

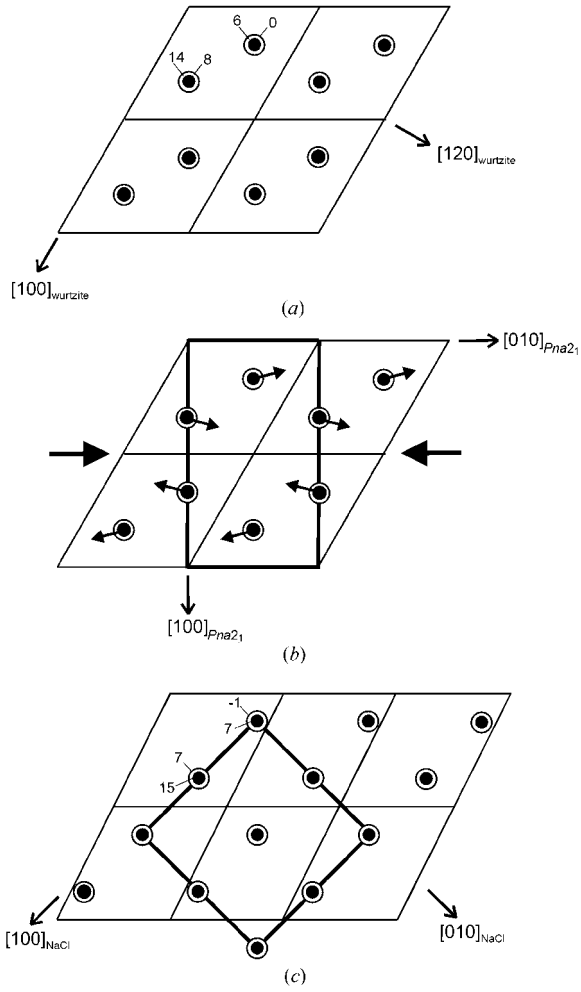

Figure 4
Schematic representation of the proposed mechanism for the wurtzite- to NaCl-type transition in $Pna2_1$. The *z* coordinates of the atoms are given in *n*/16. (*a*) Atomic arrangement of a wurtzite-type structure. (*b*) Necessary structural changes: small arrows indicate the atomic movements, bold arrows the metrical changes. (*c*) NaCl-type structure after the phase transition. Thin lines show the wurtzite-type unit cell, heavy lines that of the NaCl type (the origin is shifted by $z = \frac{1}{16}$).

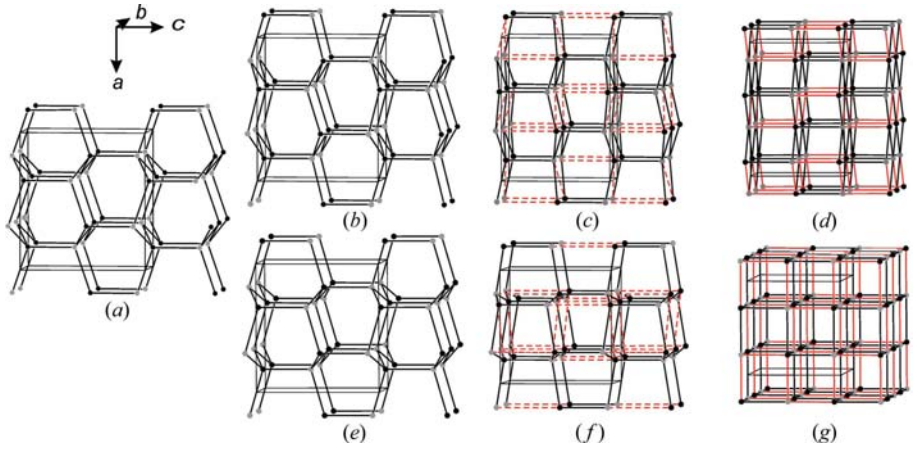

Figure 5
Schematic representation of the structural variations during the transformation from the wurtzite to the NaCl type. (*a*) Ideal wurtzite-type structure in $Pna2_1$ with $a/b = \sqrt{3}$, $c/b = \frac{2}{3}\sqrt{6}$: atoms at 4(*a*) *x*, *y*, *z* with $x = \frac{1}{3}$, $y = 0$, $z = -\frac{1}{16}$ and with $x = \frac{1}{3}$, $y = 0$, $z = \frac{9}{16}$. (*b*) Intermediate structure with symmetry $Pna2_1$ ($a/b = 1.8735$, $c/b = 1.5870$): atoms at 0.3426, 0.075, −0.0515 and at 0.3426, 0.075, 0.5515. (*c*) Intermediate structure with symmetry $Pna2_1$ ($a/b = 1.9774$, $c/b = 1.5036$): atoms at 0.3587, 0.175, −0.0228 and at 0.3587, 0.175, 0.5288. (*d*) Ideal NaCl-type structure in $Pna2_1$ ($a/b = 2$, $c/b = \sqrt{2}$): atoms at $\frac{3}{8}, \frac{1}{4}, 0$ and at $\frac{3}{8}, \frac{1}{4}, \frac{1}{2}$. (*e*) Intermediate structure with symmetry $Cmc2_1$ described in $Pna2_1$ ($a/b = 1.5076$, $c/b = 1.4473$): atoms at 0.32, 0, −0.0547 and at 0.32, 0, 0.5547. (*f*) Intermediate structure with symmetry $Cmc2_1$ described in $Pna2_1$ ($a/b = 1.2127$, $c/b = 1.1970$): atoms at 0.29, 0, −0.0345 and at 0.29, 0, 0.5345. (*g*) Ideal NaCl-type structure in $Pna2_1$ ($a/b = 1$, $c/b = 1$): atoms at $\frac{1}{4}, 0, 0$ and at $\frac{1}{4}, 0, \frac{1}{2}$. Red lines indicate the newly formed bonds in the NaCl-type structures.

Therefore, both lonsdaleite-type to *cP* transition mechanisms can be described with symmetry *Pnma* 8(*d*). The sphere-packing type 4/6/*h*2 has three degrees of freedom in the general position of *Pnma*. Fig. 3 displays the parameter region of type 4/6/*h*2 in *Pnma* 8(*d*) by a Schlegel diagram. The boundaries correspond to the parameter regions of other types of sphere packing with higher contact numbers. Table 1 lists all these sphere-packing types together with their coordinates and metrical parameters that refer to the lowest densities. Sphere packings of some of these types may also be generated with higher symmetry. In these cases, the corresponding highest symmetry and the parameter information is given in addition. As can be seen from Fig. 3 and Table 1, *cP* configurations occur twice at the boundary of the parameter region of 4/6/*h*2. For this reason, there are two different possibilities for a deformation of a lonsdaleite configuration into a packing of type 6/4/*c*1. The first transition path (Sowa,

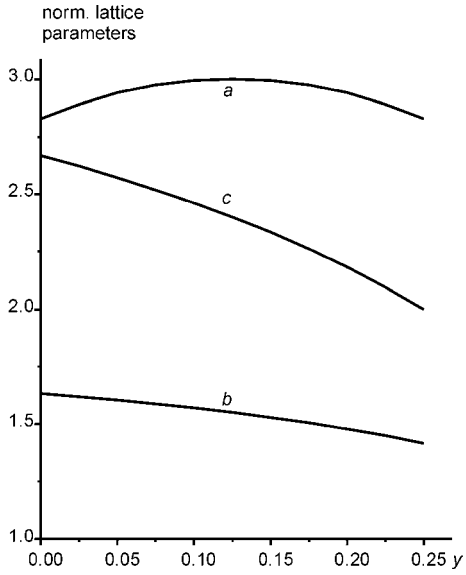

Figure 6
Variations of the normalized lattice parameters (shortest interatomic distance $d = 1$) *versus* the positional parameter *y* during the transition from the wurtzite to the NaCl type in $Pna2_1$ (transition path with ten equal distances to the next-nearest neighbours).

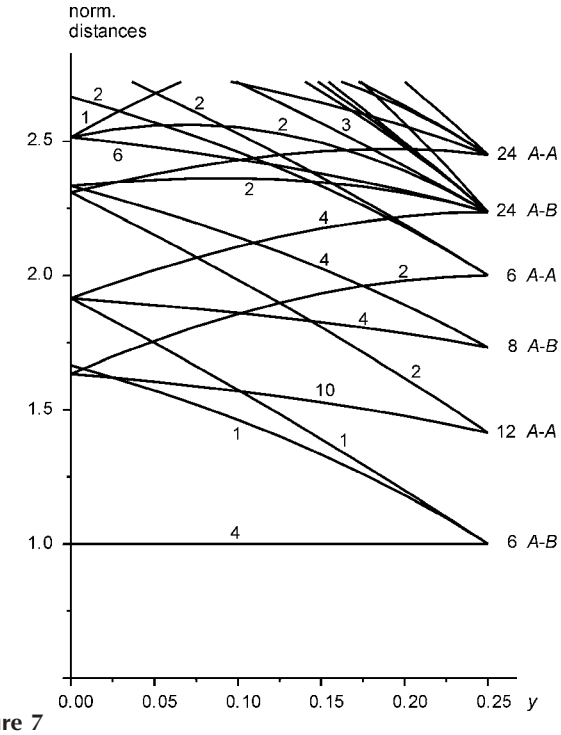

Figure 7
Variations of the normalized interatomic distances (shortest interatomic distance $d = 1$) *versus* the positional parameter *y* during the transition from the wurtzite to the NaCl type in $Pna2_1$ (transition path with ten equal distances to the next-nearest neighbours). *A*–*A* and *A*–*B* denote distances between like and unlike atoms, respectively. The numbers of equal distances are given.

2001) is characterized by atomic shifts within the plane $z = 0$. The corresponding ideal $cP(1)$ configuration occurs at 8(d) x, y, z with $x = \frac{1}{4}$, $y = 0$, $z = 0$ and $a_o = b_o = c_o = 2a_c$, $a_o/b_o = c_o/b_o = 1$. The new path leads to $cP(2)$.

It is worth noting that the structure of the hypothetical metastable h-MgO phase that has been found by Limpijumnong & Lambrecht (2001b) by using local density functional calculations corresponds to a heterogeneous sphere packing of type 5/4/h5.

Fig. 4 shows the structural changes that are necessary for the wurtzite- to NaCl-type transformation along the new path. In order to obtain an NaCl-type structure, it is not sufficient to shift the atoms parallel to [010] in the hexagonal (100) planes. Referred to the basis vectors of $P6_3mc$, the necessary total shift vector is $\pm\frac{1}{24}\sqrt{3}\mathbf{a} \pm \frac{1}{4}\mathbf{b} \pm \frac{1}{16}\mathbf{c}$. Simultaneously, the unit cell has to be contracted along the hexagonal [010] and [001] directions while the [210] direction remains unchanged. As a consequence, the following orientation relations result (*cf.* Shimojo *et al.*, 2004):

$[210]_{\rm wurtzite}$ is parallel to $[110]_{\rm NaCl}$,
$[010]_{\rm wurtzite}$ is parallel to $[\bar{1}10]_{\rm NaCl}$,
$[001]_{\rm wurtzite}$ is parallel to $[001]_{\rm NaCl}$.

In order to get an impression of the differences between the two transition mechanisms, Fig. 5 illustrates the structural deformations.

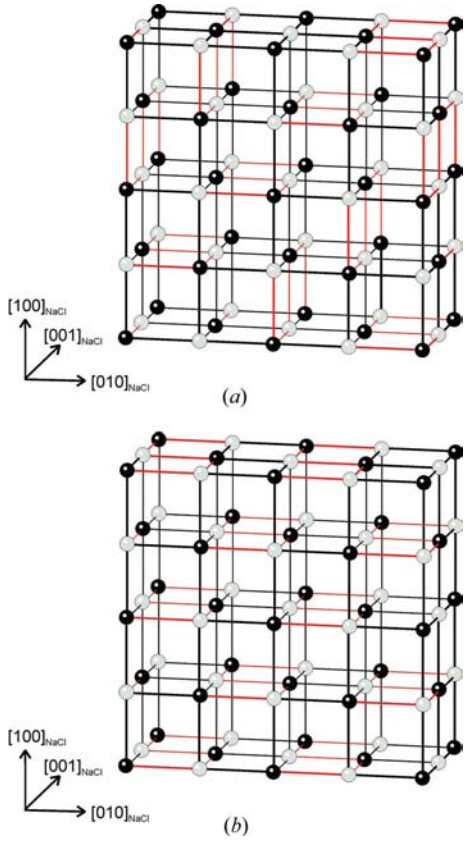

Figure 8
Pattern of breaking bonds (red) for the phase transitions from the NaCl to the wurtzite type: (*a*) $Pna2_1$ mechanism, (*b*) $Cmc2_1$ mechanism.

Shimojo *et al.* (2004) assumed for the phase transition in CdSe a two-step mechanism *via* a metastable intermediate phase with an h-MgO-type structure, but a continuous transformation from the wurtzite-type to the NaCl-type modification is just as possible.

The actual transition path, however, cannot be determined geometrically, because each line through the three-dimensional parameter region is a possible path (*cf.* Sowa, 2000*a*,*b*; 2001, 2003) if it connects the lonsdaleite and the cP configuration. A feasible restriction is that as many as possible of the next-nearest neighbours (like neighbours) of each atom should keep equal distances during the transition. In the present case, the maximal number of equidistant atoms in the second coordination shell is ten. This means that during the phase transition each kind of atom in $Pna2_1$ is arranged as a sphere packing with contact number 10. Fig. 6 shows the variations of the unit-cell parameters during the transformation for such a model. All calculations were done with normalized interatomic distances, *i.e.* the shortest distances were set to $d = 1$. The metrical alterations during a transition *via* an intermediate phase with symmetry $Pna2_1$ differ distinctly from those during a transition *via* $Cmc2_1$ (*cf.* Sowa, 2001). The lattice parameters, referred to $Pna2_1$, are $a = 2\sqrt{2} \cong 2.828$ for the wurtzite- as well as the NaCl-type structure. b changes from $\frac{2}{3}\sqrt{6} \cong 1.633$ to $\sqrt{2} \cong 1.414$, and c changes from $\frac{8}{3} \cong 2.667$ to 2. In $Cmc2_1$, the normalized lattice parameters of the wurtzite-type structure are the same as in $Pna2_1$, whereas those of the NaCl-type structure are $a = b = c = 2$.

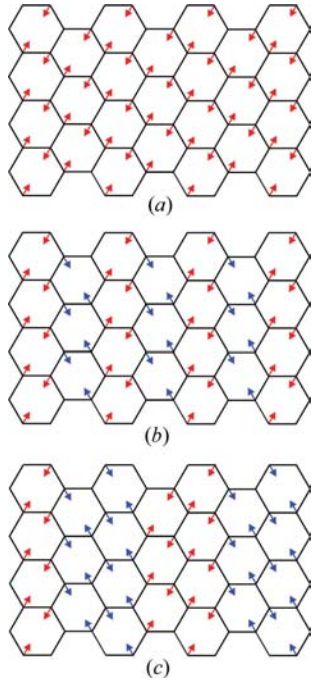

Figure 9
Schematic projection showing the atomic linkage in a wurtzite-type structure perpendicular to [001]. Red and blue arrows indicate the deformation of the hexagons and the formation of additional bonds (*a*) according to the $Cmc2_1$ mechanism, (*b*) according to the $Pna2_1$ mechanism, (*c*) according to the simplest of the possible further mechanisms.

The arrangement of one kind of atom during the newly derived phase transition in $Pna2_1$ corresponds to a sphere packing of type 10/3/*o*5. The inherent symmetry of sphere packings of this type is *Pnma* 4(*c*) $x, \frac{1}{4}, z$ with $x = \frac{3}{20}$, $z = \frac{1}{8}$ and $a/b = \frac{5}{4}$ and $c/b = \frac{1}{6}\sqrt{15}$. During the transition according to the $Cmc2_1$ mechanism, like atoms may form a sphere packing of type 10/3/*o*1 (Sowa, 2000*a*). The respective highest symmetry is *Cmcm* 4(*c*) $0, y, \frac{1}{4}$ with $y = \frac{1}{5}$ and $a/b = \frac{1}{5}\sqrt{15}$ and $c/b = \frac{2}{5}\sqrt{6}$. Both packings were described by O'Keeffe (1998).

Fig. 7 displays the variations of the normalized interatomic distances in $Pna2_1$ for the transition path with ten next-nearest neighbours. The evolution of the distances is very similar to that for the transformation *via* an intermediate structure with symmetry $Cmc2_1$ (*cf*. Sowa, 2001). Only interatomic distances longer than 2.5 show a different behaviour in the two cases. It is not surprising, therefore, that the two pathways are very similar from an energetical point of view (*cf*. Shimojo *et al.*, 2004).

Looking at the reverse transition from the NaCl to the wurtzite type, further differences between the two mechanisms become obvious: The pattern of broken bonds for the NaCl-type structures is shown in Fig. 8. In the $Cmc2_1$ mechanism, the broken bonds form meandering chains that run within one set of $\{100\}_{NaCl}$ planes, whereas in the $Pna2_1$ mechanism such chains are found within two sets of $\{100\}_{NaCl}$ planes.

By combining the two transition mechanisms, several further pathways can be modelled. One example is shown in Fig. 9 that displays a projection onto the hexagonal (001) plane. Along the $Cmc2_1$ transition path, all hexagons are deformed along the same direction (Fig. 9*a*), whereas the $Pna2_1$ mechanism requires alternating deformations in two directions (Fig. 9*b*). All further transition models also involve deformations along two directions, but the resulting unit cells have longer translation periods in one direction compared with the unit cell resulting from the $Pna2_1$ mechanism (*cf*. Fig. 9*c*). All these transitions cannot be derived from homogeneous sphere packings. The energy barriers for all these pathways are expected to be very similar. The reduction of the unit-cell volume is approximately 35% in all these cases, but owing to the longer interatomic distances in NaCl-type crystal structures the actual volume decrease in real compounds is only about 20%.

I would like to thank Professor Dr E. Koch, Marburg, for helpful discussions and the Deutsche Forschungsgemeinschaft for support of this work under KO1139/1-3.

References

Corll, J. A. (1967). *Phys. Rev.* **157**, 623–626.
Engel, P. Matsumoto, T., Steinmann, G. & Wondratschek, H. (1984). *Z. Kristallogr.* Suppl. 1.
Fischer, W. (1973). *Z. Kristallogr.* **138**, 129–146.
Fischer, W. (1991). *Z. Kristallogr.* **194**, 67–85.
Knudson, M. D., Gupta, Y. M. & Kunz, A. B. (1999). *Phys. Rev. B*, **59**, 11704–11715.
Koch, E., Fischer, W. & Müller, U. (2002). *International Tables for Crystallography*, Vol. A, 5th ed., edited by Th. Hahn, Section 15.3.5. Dordrecht/Boston/London: Kluwer Academic Publishers.
Limpijumnong, S. & Lambrecht, W. R. L. (2001*a*). *Phys. Rev. Lett.* **86**, 91–94.
Limpijumnong, S. & Lambrecht, W. R. L. (2001*b*). *Phys. Rev. B*, **63**, 104103-1–11.
Müller, U. (2004). *International Tables for Crystallography*, Vol. A1, edited by H. Wondratschek & U. Müller, Section 3.3. Dordrecht/Boston/London: Kluwer Academic Publishers.
O'Keeffe, M. (1998). *Acta Cryst.* A**54**, 320–329.
Perez-Mato, J. M., Aroyo, M., Capillas, C., Blaha, P. & Schwarz, K. (2003). *Phys. Rev. Lett.* **90**, 49603.
Sharma, S. M. & Gupta, Y. M. (1998). *Phys. Rev. B*, **58**, 5964–5971.
Shimojo, F., Ebbsjö, I., Kalia, R. K., Nakano, A., Rino, J. P. & Vashishta, P. (2000). *Phys. Rev. Lett.* **84**, 3338–3341.
Shimojo, F., Kodiyalam, S., Ebbsjö, I., Kalia, R. K., Nakano, A. & Vashishta, P. (2004). *Phys. Rev. B*, **70**, 184111-1–6.
Sowa, H. (2000*a*). *Acta Cryst.* A**56**, 288–299.
Sowa, H. (2000*b*). *Z. Kristallogr.* **215**, 335–342.
Sowa, H. (2001). *Acta Cryst.* A**57**, 176–182.
Sowa, H. (2003). *Acta Cryst.* A**59**, 266–272.
Sowa, H. (2005). *Solid State Sci.* **7**, 73–78.
Sowa, H., Koch, E. & Fischer, W. (2003). *Acta Cryst.* A**59**, 317–326.
Tolbert, S. H. & Alivisatos, A. P. (1995). *J. Chem. Phys.* **102**, 4642–4656.
Wilson, M., Hutchinson, F. & Madden, P. A. (2002). *Phys. Rev. B*, **65**, 094109-1–15.
Wilson, M. & Madden, P. A. (2002). *J. Phys: Condens. Matter*, **14**, 4629–4643.